

LiM 2011

# Dielectric Materials Volume and Surface Processing Using Femtosecond Vortex Beam

Titas Gertus<sup>a,b\*</sup>, Mindaugas Mikutis<sup>a,b</sup>, Valerijus Smilgevičius<sup>a</sup>

<sup>a</sup>Laser Research Center, Vilnius University, Sauletekio al 10, LT-10222 Vilnius, Lithuania;

<sup>b</sup>Altechna, Konstitucijos 23C, LT-08105, Vilnius, Lithuania

---

## Abstract

We demonstrate the possibility to modify dielectric materials (borosilicate glass) surface and volume using tightly focused femtosecond vortex beams (with different topological charge  $m = 1; m = 2; m = 3; m = 5; m = 10; m = 25$ ) formed by computer generated amplitude holograms. By controlling femtosecond vortex beam ( $\lambda = 1030$  nm) waist position  $\Delta z$ , number of incident pulses  $N$ , topological charge  $m$  and pulse energy  $E_p$  we get different structures induced: from micron-size ring-shaped to nano-sized structures.

*Keywords:* (320.2250) Femtosecond phenomena; (140.3390) Laser materials processing; (140.3300) Laser beam shaping; (050.4865) Optical vortices;

---

## 1. Motivation / State of the Art

Femtosecond laser vortex beam containing phase singularity and a ring-shaped beam intensity distribution can not only be used as an optical tweezers [1] or actuators for micro-electromechanical systems [2], but also for precise micromachining. Recently it was demonstrated that tightly focused femtosecond vortex laser beams can be used to ablate fused silica and soda-lime glasses [3]. Focusing a femtosecond beam into an uniaxial crystal is an efficient way to generate of optical vortices [4] and it enables enough intensity delivery to femtosecond vortex beam to be able to ablate dielectric materials. But it generates only  $m = +2$  charge vortices with limited energy. To have more energy and ability to choose topological charge, computer generated holograms [5] or phase plates [6], should be used.

## 2. Experimental

To generate femtosecond optical vortices with different topological charge ( $m = 1; m = 2; m = 3; m = 5; m = 10; m = 25$ ) we use computer generated holograms (CGH) which we fabricated using femtosecond laser PHAROS by selectively ablating thin chrome layer from glass substrate. To calculate CGH fabrication algorithm we used skeleton equation described in [0]. Fabricated CGH's are shown in Figure 1, their size there 10 mm x 10 mm, period  $A = 25$   $\mu\text{m}$ . Such amplitude CGH written in chrome on glass withstand incoming radiation intensities of

---

\* Corresponding author. Tel.: 370-5-2725738; Fax: 370-5-2723704.

E-mail address: [titas@wophotonics.com](mailto:titas@wophotonics.com).

$1.1 \cdot 10^9$  W/cm<sup>2</sup> and generate optical vortices to +1 order with efficiency of  $n = 4,63$  %.  $P_{OV} = 105$  mW is a maximum average power in femtosecond optical vortex beam we achieved. Maximum femtosecond optical vortex pulse energy at  $f = 25$  kHz is  $E_{OV} = 4$   $\mu$ J. So we are able to generate femtosecond vortex beams with peak intensities up to  $9,9 \cdot 10^7$  W/cm<sup>2</sup>.

To characterize generated femtosecond vortex beams we measured their intensity distributions with WinCamD camera (DataRay Inc.). Measured intensity distributions for different topological charge femtosecond vortex beams are shown in Figure 2. Generated vortex ring size depends not only from topological charge  $m$ , but also from the distance from hologram. Measured intensity distributions for  $m = 10$  topological charge femtosecond vortex beams at different distances from hologram are shown in Figure 3. Calculated divergence is 0,2 deg.

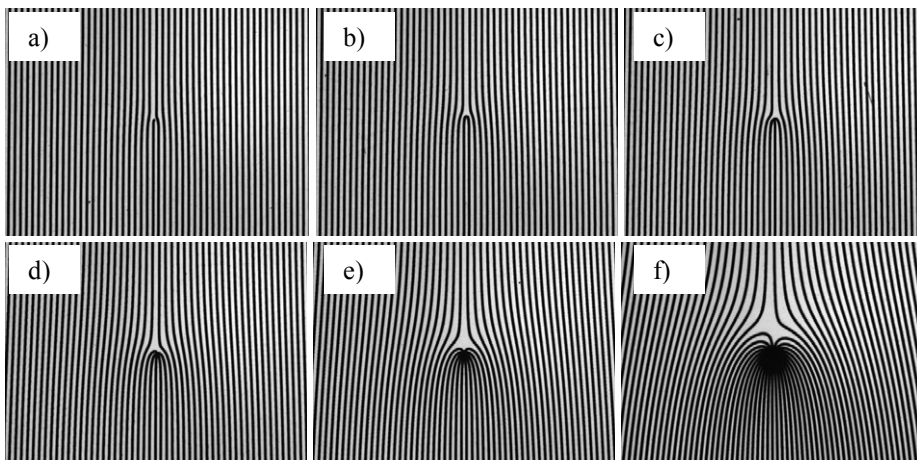


Figure 1. Computer generated holograms written in thin chrome layer on glass substrate (a)  $m = 1$ ; (b)  $m = 2$ ; (c)  $m = 3$ ; (d)  $m = 5$ ; (e)  $m = 10$ ; (f)  $m = 25$ . Period  $\Lambda = 25$   $\mu$ m. Photos were taken with optical microscope BX51 (Olympus).

We use aspheric lenses to tightly focus femtosecond vortex beams. Theoretically, in the focus we achieve femtosecond vortex beam with peak intensities up to  $6.44 \cdot 10^{14}$  W/cm<sup>2</sup>, which is equal to 200 J/cm<sup>2</sup>. We use ANT130-150 XYZ linear translation stage system (Aerotech, Inc.) to position samples and to trigger laser acousto-optic pulse picker using position synchronized output (PSO) signal.

We use a mode-locked regenerative amplified Yb:KGW (Yb-doped potassium gadolinium tungstate) femtosecond laser source with following parameters: wavelength  $\lambda = 1030$  nm, pulse duration  $\tau = 300$  fs, pulse repetition rate variable from  $f = 1$  kHz to  $f = 200$  kHz, maximum average power up to  $P = 5$  W.

In our experiments we are varying femtosecond vortex beam waist position, number of incident pulses, pulse energy and topological charge.

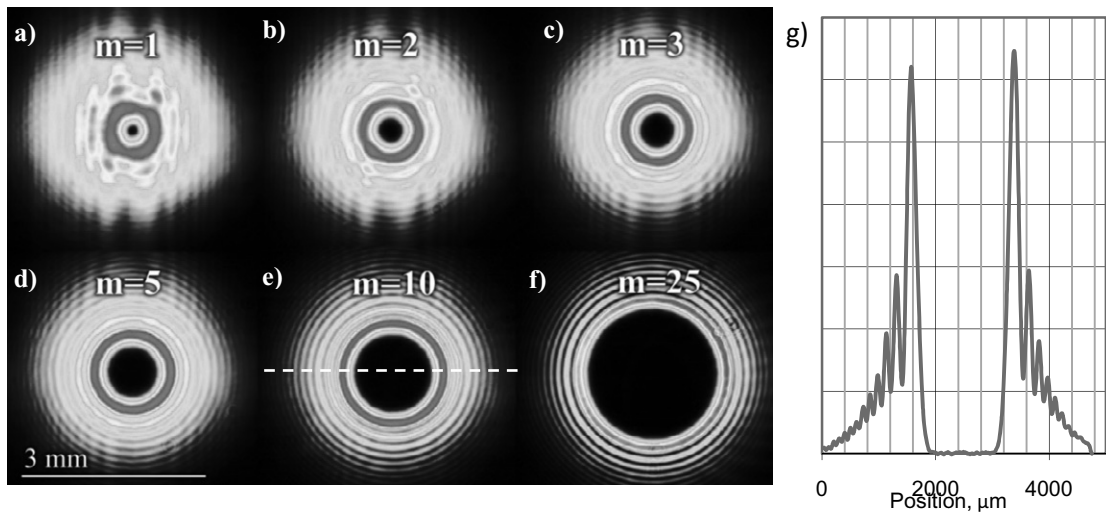


Figure 2. (a)  $m = 1$ ; (b)  $m = 2$ ; (c)  $m = 3$ ; (d)  $m = 5$ ; (e)  $m = 10$ ; (f)  $m = 25$  topological charge femtosecond vortex beam intensity distributions measured with WinCamD camera (DataRay Inc.). Distance from camera to hologram was 180 mm. (g)  $m = 10$  femtosecond vortex beam intensity distribution profile dashed line (e).

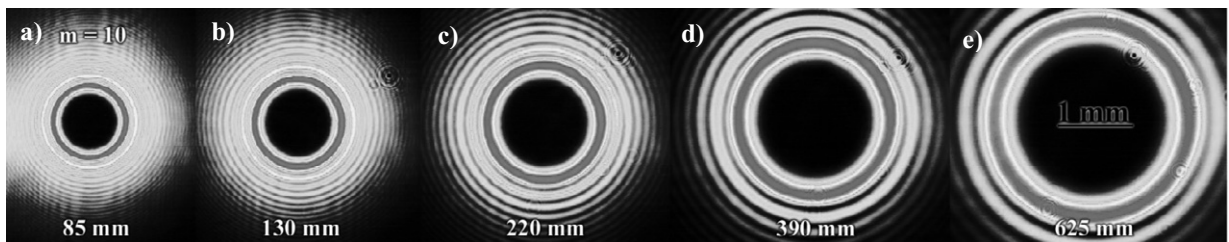


Figure 3.  $m = 10$  femtosecond vortex beam intensity distributions at different distances from grating: (a) 85 mm; (b) 130 mm; (c) 220 mm; (d) 390 mm; (e) 625 mm.

Structures induced on borosilicate glass surface using single femtosecond vortex ( $m = 1$ ) pulses with energy  $E_p = 7 \mu\text{J}$  while varying beam waist position are shown in Figure 4(a-i). We used  $f = 4.03 \text{ mm}$  focal length aspheric lens (NA = 0.62) with clear aperture of 5 mm. Induced structures shape and size greatly depends on beam waist shift  $\Delta z$ . Induced structures vary from correctly ring-shaped to multi ring. When  $\Delta z = 43 \mu\text{m}$ , induced structure size becomes  $\approx 500 \text{ nm}$ , less than wavelength  $\lambda = 1030 \text{ nm}$  used. When  $\Delta z > 45 \mu\text{m}$ , there are no more structures induced on the surface of borosilicate glass, instead we can detect volume modifications.

Different number of pulses also influence induced structure. In Figure 4(j-o) structures induced on borosilicate glass surface using different number of femtosecond vortex ( $m = 1$ ) pulses. Ring shaped structures disappear after several pulses shoot to the same place.

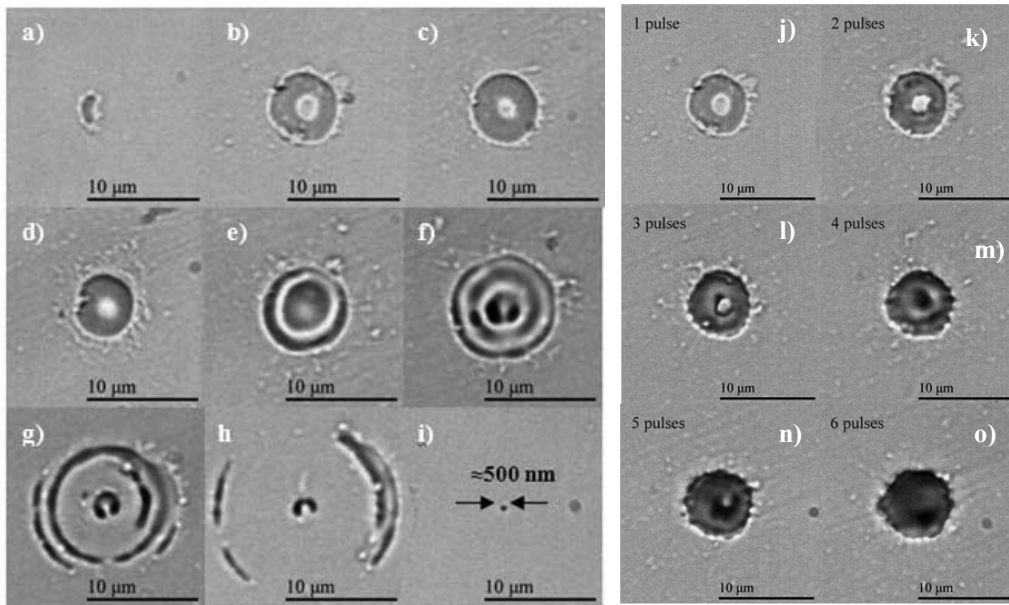


Figure 4. Structures induced on borosilicate glass surface using single femtosecond vortex ( $m = 1$ ) pulses with different beam waist shift (a)  $\Delta z = 1 \mu\text{m}$ ; (b)  $\Delta z = 6 \mu\text{m}$ ; (c)  $\Delta z = 11 \mu\text{m}$ ; (d)  $\Delta z = 16 \mu\text{m}$ ; (e)  $\Delta z = 21 \mu\text{m}$ ; (f)  $\Delta z = 26 \mu\text{m}$ ; (g)  $\Delta z = 31 \mu\text{m}$ ; (h)  $\Delta z = 36 \mu\text{m}$ ; (i)  $\Delta z = 43 \mu\text{m}$ . Structures induced on borosilicate glass surface using different number of femtosecond vortex ( $m = 1$ ) pulses: (j)  $N = 1$ ; (k)  $N = 2$ ; (l)  $N = 3$ ; (m)  $N = 4$ ; (n)  $N = 5$ ; (o)  $N = 6$ .

To demonstrate different topological charge femtosecond single pulse induced structures, we fabricate thin chrome layer on glass substrate instead of borosilicate glass. Because,  $m > 3$  topological charge femtosecond vortices ring don't carry enough peak energy to damage glass surface even if they have same average power. Structures induced in thin chromium layer using single femtosecond vortex pulses ( $\lambda = 1030 \text{ nm}$ ;  $P = 100 \text{ mW}$ ;  $f = 50 \text{ kHz}$ ) with different topological charge ( $m = 1$ ;  $m = 2$ ;  $m = 3$ ;  $m = 5$ ;  $m = 10$ ;  $m = 25$ ) are shown in Figure 5. Figure 5g shows  $m = 25$  single femtosecond vortex pulse induced  $23 \mu\text{m}$  diameter ring shaped structure with  $2 \mu\text{m}$  ring width.

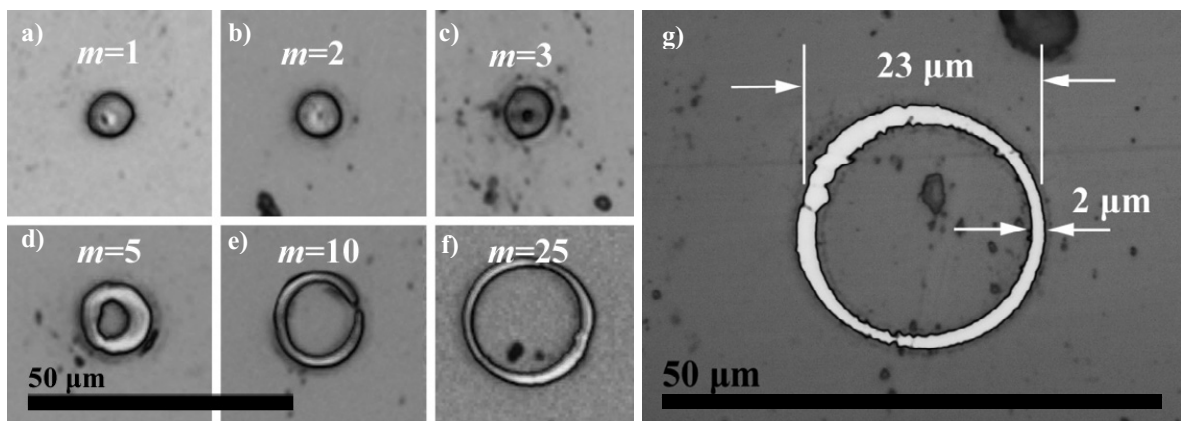


Figure 5. Structures ablated in thin chromium layer using single femtosecond vortex pulses ( $\lambda = 1030 \text{ nm}$ ;  $P = 100 \text{ mW}$ ;  $f = 50 \text{ kHz}$ ) with different topological charge (a)  $m = 1$ ; (b)  $m = 2$ ; (c)  $m = 3$ ; (d)  $m = 5$ ; (e)  $m = 10$ ; (f)  $m = 25$  (g) zoomed  $m = 25$ .

We used  $f = 6.24 \text{ mm}$ ,  $\text{NA} = 0.42$  aspheric lens to demonstrate femtosecond vortex beam cutting possibilities. Grooves made on borosilicate glass surface using focused femtosecond optical vortex beam ( $\lambda = 1030 \text{ nm}$ ;

$P = 100$  mW;  $f = 50$  kHz; pulse density 10000 pulses/mm) with different topological charge are shown in Figure 6. Comparing grooves made with Gaussian and different topological charge femtosecond vortex beams, it is clear that grooves made using Gaussian beam are narrower and have better quality. We were not able to ablate borosilicate glass surface with  $m = 10$  and  $m = 25$ , as such beam ring peak intensity is too low. As seen in Figure 6(e),  $m = 5$  femtosecond vortex beam also has a great reduction in peak intensity, as ablated groove is smaller even than  $m = 3$ . Figure 6g shows 5  $\mu$ m diameter modifications made in volume of borosilicate glass using femtosecond vortex beam with topological charge  $m = 2$ .

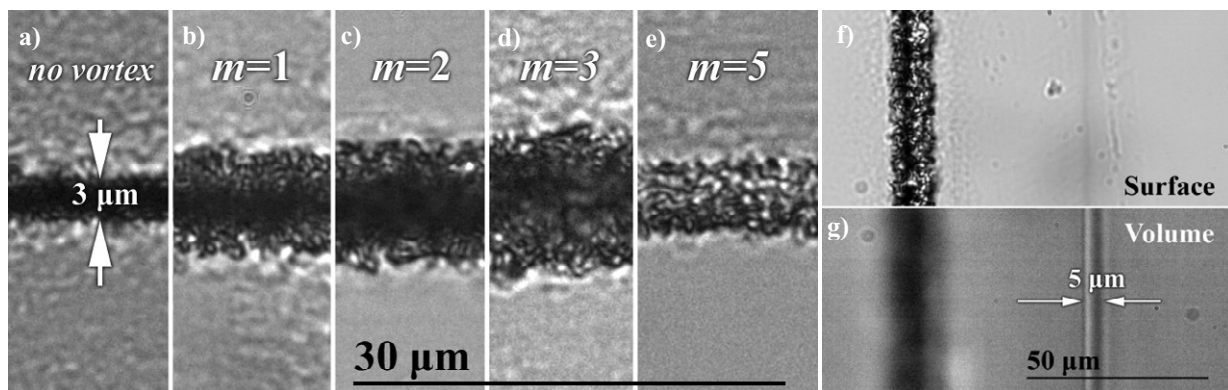


Figure 6. Cuts made on borosilicate glass surface using focused femtosecond optical vortex beam ( $\lambda = 1030$  nm;  $P = 100$  mW;  $f = 50$  kHz; pulse density was 10000 pulses/mm) with different topological charge: (a) Gaussian beam (b)  $m = 1$ ; (c)  $m = 2$ ; (d)  $m = 3$ ; (e)  $m = 5$ . Cut made inside volume of borosilicate glass using femtosecond vortex beam with topological charge  $m = 2$  (f) camera focus on borosilicate glass sample surface (g) camera focus inside volume.

### 3. Conclusions

Structures induced on borosilicate glass surface and thin chromium layer using single femtosecond vortex pulses highly depend on beam waist position, number of pulses, pulse energy and topological charge. We show the possibility to fabricate nano-meter sized structures ( $\approx 500$  nm) which size is less than wavelength ( $\lambda = 1030$  nm) used. Also we show the possibility to fabricate dielectric material volume using femtosecond vortex beams.

Therefore we were not able to machine high-quality micron-size ring-shaped structures with less than 100 nm uniform groove thickness as showed in [3]. This is probably because we use lower NA focusing lens, longer pulses and amplitude CGH used is inherently chromatic and therefore require the introduction of correcting elements in order to compensate topological charge dispersion occurring in femtosecond pulses.

### References

- [1] Gahagan, K. T. & Swartzlander, G. A. Trapping of low-index microparticles in an optical vortex. *J. Opt. Soc. Am. B* 15, 524–534 (1998).
- [2] M. E. J. Friese, H. Rubinsztein-Dunlop, J. Gold, P. Hagberg and D. Hanstorp, *Appl. Phys. Lett.* 78, 547 (2001).
- [3] Cyril Hnatovsky, Vladlen G. Shvedov, Wieslaw Krolikowski, and Andrei V. Rode, "Materials processing with a tightly focused femtosecond laser vortex pulse," *Opt. Lett.* 35, 3417-3419 (2010).
- [4] V. G. Shvedov, C. Hnatovsky, W. Krolikowski, A. V. Rode, "Efficient Beam Converter for the Generation of Femtosecond Vortices," arXiv:1005.1470v1, (2010).
- [5] Carpentier, Alicia V.; Michinel, Humberto; Salgueiro, José R.; Olivieri, David, Making optical vortices with computer-generated holograms, *American Journal of Physics*, Volume 76, Issue 10, pp. 916-921 (2008).
- [6] S. S. R. Oemrawsingh, J. A. W. van Houwelingen, E. R. Eliel, J. P. Woerdman, E. J. K. Versteegen, J. G. Kloosterboer, and G. W. Hooft, Production and Characterization of Spiral Phase Plates for Optical Wavelengths, *Applied Optics*, Vol. 43, Issue 3, pp. 688-694 (2004)
- [7] James Strohaber, Timothy D. Scarborough, and Cornelis J. G. J. Uiterwaal, Ultrashort intense-field optical vortices produced with laser-etched mirrors, *APPLIED OPTICS*, Vol. 46, No. 36, 20 December 2007.